

## **Anonymous Referee #1**

We would like to thank the reviewer for her/his positive evaluation and the very helpful comments and suggestions. Below we reply on each specific comment.

- 119 "the exponent was fixed to 0.5" could you please better explain why and for what this exponent stands, I am not sure every reader would know.

Reply: We added the following information to the ms:

“The Schmidt-number exponent  $n$  describes the dependence of the gas exchange velocity of a particular gas on the diffusion coefficient of this gas in water. We used  $n=0.5$ , which showed best agreement with measurements for wave-covered and turbulent water surfaces (Jähne and Haußecker, 1998).

- 337 I find a difference in flow of only 0.02 between left and middle very minor, is this correct or wrong spelled/written? Shouldn't the difference between those both speeds more?

Reply: The flow velocities refer to the mean flow velocities in the flume, without chamber-induced disturbances, and are correct. Due to technical limitations, we could only use a rather narrow range of flow velocities in the flume.

- 39 velocity can also be derived

- 45 presence

- 115 comma instead of point

- 225 delete one "however"

- 298 for up to 5 minutes every 30s: seems difficult for me or do not understand

- 322 reference after point Fig. 1 "The solid line shows..."

Reply: These typos were corrected.

## **Anonymous Referee #2**

Reply: We would like to thank the reviewer for her/his positive evaluation and the very helpful comments and corrections. Below we reply on each specific comment.

- Abstract – in the list of four points made from this study, switch numbers 1 and 2 so that you start by stating that anchored chambers produce turbulence. It seems to make more sense to start by saying that you find something in one method and then that you didn't in the other, instead of the other way around.

Reply: We followed the reviewer's suggestion and changed the abstract accordingly.

- P14622, L19-22 – I am not sure if this sentence regarding microbubbles fits here, especially since the papers you cited refer to lakes. Perhaps you can be clearer with what you are trying to convey with this point and you could use Beaulieu 2012 as a better reference for elevated  $k_{CH_4}$  in rivers.

Reply: The sentence was changed to: "Moreover, recent studies revealed that the gas exchange velocity of  $CH_4$  can be enhanced by microbubbles (Beaulieu et al., 2012) and can therefore differ from that of the volatile tracer."

- P14623, L8 – Vachon et al. 2010 also discusses turbulence bias of chambers

Reply: We relate our findings to the study of Vachon (which refers to lakes and reservoirs) in the discussion section.

P14624, L6-7 – Change 'produced' to 'produce' and add a question mark at the end of the question.

Reply: Corrected.

- P14624, L8 – More details should be give about the size or stream order of the 9 rivers, especially since Hotchkiss et al 2015 just found that  $CO_2$  emissions change with size of streams. This new article should be cited and discussed in your manuscript. (Hotchkiss, E. R., Hall Jr, R. O., Sponseller, R. A., Butman, D., Klaminder, J., Laudon, H., ... & Karlsson, J. (2015). Sources of and processes controlling  $CO_2$  emissions change with the size of streams and rivers. *Nature Geoscience*, 8(9), 696-699.)

Reply: Information on discharge are now provided in Table 2.

We now refer to the new article in our introduction section. Because the major purpose of the present manuscript is on methodological issues, we consider a more detailed discussion of the magnitude of the observed fluxes and their relation to controlling processes at the landscape scale is not appropriate.

- P14623, L12-17 – Does using these different methods influence your flux results? I presume not seeing as what is important is the rate of accumulation and not absolute concentrations; however, you should make this clear in the text as it may cause confusion.

Reply: We assume the reviewer is referring to p. 14624. The uncertainties related to the relative accuracy of the different instruments is small compared to differences observed between different deployment types.

- P14625, L9 – add '(F)' after 'fluxes' to define the variable in eq.3

Reply: The flux symbol F is defined before, above Eq. 1.

- P14626, L20-25 – this section is a bit hard to follow. Is it possible to include a supplemental figure that will help the reader understand this process?

Reply: We did not find an intuitive way to illustrate this procedure in a figure. The text was changed to:

“The longitudinal extent of the observed flow fields (433 mm for anchored and 395 mm for drifting chambers) covered the complete chamber diameter and velocities are reported as a function of distance from the leading chamber edge in both the anchored and the drifting deployment.”

- P14627, L15 – delete 'measured'

- P14628, L6-7 – rewrite 'than those under drifting chambers, with individual measurements of k600\_CO2\_a being up to 20 times higher than k600\_CO2\_d. The average ratio'

Reply: We applied the suggested changes.

- Figures 2a and b can have fit lines that refer to those discussed on P14628, L20 & L23

A fit line was added to Fig. 2b only. We realized that the individual fit lines for the various data sets in in Fig. 2a would add too much complexity to the figure and decided to skip these in favor of clarity.

Technical Note: Drifting versus anchored flux chambers for measuring  
greenhouse gas emissions from running waters

Andreas Lorke<sup>1\*</sup>, Pascal Bodmer<sup>2,3</sup>, Christian Noss<sup>1</sup>, Zeyad Alshboul<sup>1</sup>, Matthias  
Koschorreck<sup>4</sup>, Celia Somlai-Haase<sup>1</sup>, David Bastviken<sup>5</sup>, Sabine Flury<sup>2</sup>, Daniel F. McGinnis<sup>2,6</sup>,  
Andreas Maeck<sup>7</sup>, Denise Müller<sup>8,9</sup>, Katrin Premke<sup>2,10</sup>

<sup>1</sup> Institute for Environmental Sciences, University of Koblenz-Landau, Fortstr. 7, 76829  
Landau, Germany

<sup>2</sup> Leibniz-Institute of Freshwater Ecology and Inland Fisheries, Chemical Analytics and  
Biogeochemistry, Müggelseedamm 310, 12587 Berlin, Germany

<sup>3</sup> Institute of Biology, Freie Universität Berlin, Berlin, Germany

<sup>4</sup> Helmholtz Centre for Environmental Research – UFZ, Department Lake Research,  
Brückstr.3a, 39114 Magdeburg, Germany

<sup>5</sup> Linköping University, Department of Thematic Studies – Environmental Change, 58183  
Linköping, Sweden,

<sup>6</sup> Institute F.-A. Forel, Section of Earth and Environmental Sciences, University of Geneva,  
Geneva, Switzerland

<sup>7</sup> Senect GmbH & Co. KG, An 44 – No. 11, 76829 Landau, Germany

<sup>8</sup> Institute of Environmental Physics (IUP), Otto-Hahn-Allee 1, 28359 Bremen, Germany

<sup>9</sup> Center for Tropical Marine Ecology (ZMT), Fahrenheitstr. 8, 28359 Bremen, Germany

<sup>10</sup> Leibniz Centre for Agricultural Landscape Research, Institute for Landscape  
Biogeochemistry, Eberswalder Straße 84, 15374 Müncheberg, Germany

\* Corresponding author: [lorke@uni-landau.de](mailto:lorke@uni-landau.de)

Feldfunktion geändert

## Abstract

1 Stream networks were recently discovered as major but poorly constrained natural greenhouse  
2 gas (GHG) sources. A fundamental problem is that several measurement approaches have  
3 been used without cross comparisons. Flux chambers represent a potentially powerful  
4 methodological approach if robust and reliable ways to use chambers on running water can be  
5 defined. Here we compare the use of anchored and freely drifting chambers on various  
6 streams having different flow velocities. The study clearly shows that (1) anchored chambers  
7 enhance turbulence under the chambers and thus elevate fluxes, (2) drifting chambers have a  
8 very small impact on the water turbulence under the chamber and thus generate more reliable  
9 fluxes, (3) the bias of the anchored chambers greatly depends on chamber design and  
10 sampling conditions, and (4) there is a promising method to reduce the bias from anchored  
11 chambers by using a flexible plastic foil seal to the water surface rather than having rigid  
12 chamber walls penetrating into the water. Altogether, these results provide novel guidance on  
13 how to apply flux chambers in running water, which will have important consequences for  
14 measurements to constrain the global GHG balances.

**Gelöscht:** drifting chambers have a very small impact on the water turbulence under the chamber and thus generate more reliable fluxes

**Gelöscht:** anchored chambers enhance turbulence under the chambers and thus elevate fluxes

## 19 1 Introduction

20 Rivers and streams have been identified as important links in the global carbon cycle. They  
21 receive and transport terrestrial carbon from the land to the ocean and are also shown to be a  
22 net source of greenhouse gases (GHG), i.e carbon dioxide (CO<sub>2</sub>) and methane (CH<sub>4</sub>)  
23 (Aufdenkampe et al., 2011; Battin et al., 2008; Cole et al., 2007; Tranvik et al., 2009). In a  
24 recent study, the global CO<sub>2</sub> emissions from rivers and streams were estimated to be 1.8±0.25  
25 Gt C year<sup>-1</sup> (Raymond et al., 2013), which corresponds to 70% of the global ocean carbon  
26 sink (Le Quéré et al., 2014). Due to the lack of knowledge of surface area and gas exchange  
27 velocity, the smallest streams are considered as a major unknown component of regional to  
28 global scale GHG emission estimates (Bastviken et al., 2011; Cole et al., 2007). Despite these  
29 knowledge gaps, there are strong indications that small streams have the highest gas exchange  
30 velocities (Aufdenkampe et al., 2011), highest CO<sub>2</sub> partial pressures (Koprivnjak et al., 2010)  
31 and cover the largest fractional surface area within fluvial networks (Butman and Raymond,  
32 2011). [A continental-scale analysis of CO<sub>2</sub> efflux from streams and rivers revealed a](#)  
33 [continuous decline of the fluxes with increasing size and discharge of the aquatic systems](#)  
34 (Hotchkiss et al., 2015).  
35 Ecosystem-scale fluxes of CO<sub>2</sub> and CH<sub>4</sub> from running waters are often derived indirectly  
36 using measured gas partial pressure in the surface water in combination with estimates of a  
37 gas exchange velocity. For sparingly soluble gases, the exchange velocity is mainly controlled  
38 by turbulence at the water-side of the air-water interface. In smaller rivers and streams,  
39 turbulence is driven by stream velocity, depth and bottom roughness (Marion et al., 2014),  
40 and the resulting gas exchange velocities are often parameterized with one or more of the  
41 following terms: stream order, slope, [flow velocity](#), discharge, width and depth (Alin et al.,  
42 2011; Raymond et al., 2012; Wallin et al., 2011). In small streams, reach-scale estimates of the  
43 gas exchange velocity can also be derived from gas tracer experiments, whereby a volatile

Formatiert: Tiefgestellt

44 tracer (e.g., propane or sulfur hexafluoride) is injected upstream and the longitudinal decrease  
45 of its dissolved concentration is measured (Halbedel and Koschorreck, 2013; Raymond et al.,  
46 2012). For practical reasons, tracer gas injections are limited to application in small streams  
47 and alternative methods suitable for a greater range of stream sizes are needed. Moreover,  
48 recent studies revealed that the gas exchange velocity of CH<sub>4</sub> can be enhanced by  
49 microbubbles (Beaulieu et al., 2012) and can therefore differ from that of the volatile tracer. To  
50 better constrain ecosystem-scale estimates of GHG emissions and to improve the  
51 understanding of the flux drivers in small running waters, reliable methods are required that  
52 allow direct measurements.  
53 As eddy-covariance (Baldocchi, 2014) measurements are not suitable for small streams, gas  
54 flux chambers that float on the water surface are a straightforward and inexpensive method  
55 for direct measurements of gas fluxes, and can easily be replicated over time and space  
56 (Bastviken et al., 2015). The gas flux is determined from the change of the gas concentration  
57 in the chamber headspace over time. Floating chambers have been frequently applied for  
58 measuring gas fluxes in large rivers, reservoirs and lakes (e.g., Beaulieu et al.,  
59 2014; DelSontro et al., 2011; Eugster et al., 2011).  
60 Chamber measurements have been criticized because submerged chamber edges are thought  
61 to disrupt the aquatic boundary layer, thereby affecting the gas exchange (Kremer et al.,  
62 2003). Comparisons of floating chambers with other flux measurement techniques were  
63 performed in lakes, rivers and estuaries. While some studies have reported a tendency of  
64 floating chambers to yield higher fluxes than other methods (Raymond and Cole,  
65 2001; Teodoru et al., 2015), others found reasonable agreement (Gålfalk et al., 2013; Cole et  
66 al., 2010).  
67 In streams and rivers, floating chambers have been deployed anchored at one spot (anchored  
68 chambers) (Sand-Jensen and Staehr, 2012; Crawford et al., 2013), or freely drifting with the  
69 water (drifting chambers) (Alin et al., 2011; Beaulieu et al., 2012). Although based on the

**Gelöscht:** y

**Gelöscht:** significantly larger

**Gelöscht:** than that of CO<sub>2</sub>, which has been attributed to the presence of microbubbles (McGinnis et al., 2014; Prairie and del Giorgio, 2013)

75 same principle, the two deployment modes have fundamental differences. Because of the  
76 higher velocity difference between the chamber and the surface water, anchored chambers in  
77 running waters may create additional turbulence around the chamber edges (Kremer et al.,  
78 2003). ~~If~~ the effect of this turbulence on fluxes is minor, anchored chambers would be  
79 advantageous as the area covered by the chamber can be controlled and because practical  
80 work with anchored chambers is relatively simple. Drifting chambers will likely induce less  
81 turbulence in the surface water, however it is difficult to control their coverage, potentially  
82 resulting in spatially biased measurements. Drifting chambers are also complicated for several  
83 reasons, e.g., the presence of obstacles in the streams or in terms of logistics, as the chambers  
84 may travel far during measurement periods.

85 While establishing efficient methods for running water gas emissions are needed to improve  
86 the global GHG budgets, progress in chamber based methods is prevented by the lack of  
87 comparative assessments of anchored versus drifting chambers. In this study, we compared  
88 measurements of GHG fluxes and the gas exchange velocity using drifting and anchored  
89 chambers in various streams and rivers. Because chamber performance is expected to depend  
90 strongly on chamber design, the field experiments were conducted using three different  
91 chamber types. In laboratory experiments, we analyzed the flow field and the turbulence  
92 under both anchored and drifting chambers at different flow velocities. The primary objective  
93 of this study was to answer the question: Do anchored chambers produce ~~reliable~~  
94 measurements of localized GHG fluxes in running waters?

## 95 2 Methods

### 96 2.1 Chamber measurements in the field

97 Field measurements were conducted in nine different rivers and streams in Germany and  
98 Poland using three different chambers ([Table 1](#)). All three data sets included *anchored*  
99 *measurements*, where the chambers were tethered to stay at a fixed position as well as *drifting*

Gelöscht: However, i

Gelöscht: d

Gelöscht: .

Feldfunktion geändert



103 *measurements*, where the chambers were freely moving with the current. In two of the data  
104 sets (A and B), the temporal change of CO<sub>2</sub> and CH<sub>4</sub> concentration in the chamber headspace  
105 was measured on a boat using infrared gas analyzers (A: OA-ICOS gas analyzer, UGGA, Los  
106 Gatos Research Inc. USA, B: FTIR analyzer, Gasetm 4010, Gasetm, Finland). In the third  
107 data set (C), the gas concentration was measured using a built-in and low-cost CO<sub>2</sub> sensor  
108 (ELG, SenseAir, Sweden). The chamber used in (C) is described in detail elsewhere  
109 (Bastviken et al., 2015).

110 The chamber flux measurements were supplemented by measurements of dissolved gas  
111 concentrations (CO<sub>2</sub> and in data set A and B also CH<sub>4</sub>) in the stream water and in the  
112 atmosphere ([Table 1](#)). Additional measurements include water temperature and near-surface  
113 current velocity, which was measured at selected sites within the study reaches using acoustic  
114 or electromagnetic current meters. More details on sampling and instrumentation are provided  
115 in [Appendix A](#).

116 The flux  $F$  (mmol m<sup>-2</sup> d<sup>-1</sup>) of CO<sub>2</sub> (all data sets) and CH<sub>4</sub> (parts of data set A and B), was  
117 calculated from the observed rate of change of the mole fraction  $S$  (ppm s<sup>-1</sup>) of the respective  
118 gas in the chamber using (Campeau and Del Giorgio, 2014):

$$119 \quad F = (S \cdot V / A) \cdot t_1 \cdot t_2 \quad (1)$$

120 Where  $V$  is the chamber gas volume (m<sup>3</sup>),  $A$  is the chamber area (m<sup>2</sup>),  $t_1=8.64 \times 10^4$  s d<sup>-1</sup> is the  
121 conversion factor from seconds to days, and  $t_2$  is a conversion factor from mole fraction  
122 (ppm) to concentration (mmol m<sup>-3</sup>) at *in-situ* temperature ( $T$  in K) and atmospheric pressure ( $p$   
123 in Pa), according to the ideal gas law:

$$124 \quad t_2 = p / (8.31 \text{ J K}^{-1} \text{ mole}^{-1} \cdot T) \cdot 1000 \quad (2)$$

125 The gas exchange velocity of the respective gas at *in-situ* temperature  $k$  (m d<sup>-1</sup>) was estimated  
126 from measured fluxes as:

$$127 \quad k = F / (K_H \cdot (p^{\text{water}} - p^{\text{air}})) \quad (3)$$

Feldfunktion geändert

Feldfunktion geändert

128 using the partial pressure of CO<sub>2</sub> and CH<sub>4</sub> in the stream water ( $p^{water}$ ) and in the atmosphere  
129 ( $p^{air}$ ). The partial pressures were obtained by multiplication of the measured mole fraction  
130 with atmospheric pressure.  $K_H$  is the temperature-dependent Henry constant (mmol m<sup>-3</sup> Pa<sup>-1</sup>)  
131 (Goldenfum, 2011). The *in-situ* gas exchange velocities were converted to a standardized  
132 (independent of temperature and gas diffusivity) exchange velocity  $k_{600}$  using the Schmidt  
133 number dependence:

$$k_{600} = k \cdot (600 / Sc)^n \quad (4)$$

134 where the temperature-dependent Schmidt numbers ( $Sc$ ) of both gases were estimated  
135 according to Goldenfum (2011). The Schmidt-number exponent  $n$  describes the dependence  
136 of the gas exchange velocity of a particular gas on the diffusion coefficient of this gas in  
137 water. We used  $n=0.5$ , which showed best agreement with measurements for wave-covered  
138 and turbulent water surfaces (Jähne and Haußecker, 1998).

Gelöscht: was

Gelöscht: fixed at

Formatiert: Schriftart: Kursiv

140

## 141 2.2 Turbulence measurements in the lab

142 The flow fields under freely drifting and anchored chambers were measured using particle  
143 image velocimetry (PIV) in a 3 m long laboratory flume. The chamber type and geometry was  
144 identical to the chamber in data set C (Table 1). The flow field under the drifting chamber was  
145 measured for 50 repeated chamber runs (58 s cumulative velocity observations under the  
146 chamber) at a mean flow velocity of 0.10 m s<sup>-1</sup>, the highest flow velocity that could be  
147 realized in the flume. Measurements under anchored chambers were performed for 90 s at a  
148 mean flow velocity of 0.10 m s<sup>-1</sup>. Additional measurements were performed at reduced mean  
149 flow velocities of 0.08 and 0.06 m s<sup>-1</sup>. As a reference, the undisturbed flow field without  
150 chambers was measured for 90 s. Due to the limited length of the laboratory flume it was not  
151 possible to measure gas fluxes or estimate the gas exchange velocities.

Feldfunktion geändert

152 The flow fields were analyzed by illuminating neutrally buoyant seeding particles (diameter  
153 of 20 µm, polyethylene) within a thin light sheet produced by a double-pulse laser

156 (DualPower 200-15, DantecDynamics) with 5 ms between pulses. The sampling frequency  
157 was 7.5 Hz. Images were recorded in a  $145 \times 145 \text{ mm}^2$  field of view with a charge-coupled  
158 device (CCD) camera (FlowSense 4M MKII,  $2048 \times 2048$  pixels, DantecDynamics). The  
159 camera was inclined by  $30^\circ$  to the horizontal, which allowed for observing flow velocities  
160 below the chamber.

161 The two-dimensional (longitudinal and vertical) flow velocities within the field of view were  
162 estimated using an adaptive correlation algorithm (Dynamic Studio, DantecDynamics) with a  
163 final spatial resolution of  $2.6 \times 2.6 \text{ mm}^2$ . The longitudinal extent of the observed flow fields  
164 ( $433 \text{ mm}$  for anchored and  $395 \text{ mm}$  for drifting chambers) covered the complete chamber  
165 diameter and velocities are reported as a function of distance from the leading chamber edge  
166 in both the anchored and the drifting deployment.

167 The turbulent kinetic energy (*TKE*) was estimated by assuming isotropy in the unresolved  
168 velocity component as:

169 
$$TKE = \frac{3}{4} \overline{(u'^2 + w'^2)} \quad (5)$$

170 where  $u'$  and  $w'$  denote the temporal fluctuations of the longitudinal and vertical velocity  
171 component, respectively, and the overbar denotes temporal averaging.

## 172 2.3 Statistics

173 The mean fluxes measured with anchored and drifting chambers in the respective field data  
174 sets were compared using paired *t*-tests, comparisons between the data sets were performed  
175 using 2-sample *t*-tests. Spearman rank correlations coefficients ( $r_s$ ) were estimated when  
176 testing for correlations between gas exchange velocities from anchored and drifting chambers  
177 for each data set. All analyses were performed at a significance level  $p < 0.05$ , unless stated  
178 otherwise.

Gelöscht: Longitudinally extended

Gelöscht: .

Gelöscht: These flow fields were composed from individual observations by assembling the velocity vectors relative to the (moving) leading edge of the chamber.

Gelöscht:  $TKE = \frac{3}{4} \overline{(u'^2 + w'^2)}$

## 185 3 Results

### 186 3.1 Drifting vs. anchored chamber measurements in the field

187 In all measurements, the  $\text{CO}_2$  and  $\text{CH}_4$  fluxes were positive, i.e. the streams were sources of  
188 both gases to the atmosphere. While the mean  $\text{CO}_2$  fluxes measured by drifting chambers did  
189 not differ significantly among the data sets B and C, they were about seven-fold higher in data  
190 set A (Table 2). In all data sets, anchored chamber fluxes were significantly higher than the  
191 corresponding drifting chamber fluxes.

192 Gas exchange velocities  $k_{600}$  estimated from  $\text{CO}_2$  measurements in the drifting chamber  
193 deployments ( $k_{600\_CO2\_d}$ ) ranged between 0.2 and 8.1  $\text{m d}^{-1}$ . They varied widely within each  
194 data set (Table 2), but in contrast to the current velocities mean values of  $k_{600\_CO2\_d}$  did not

195 significantly differ among the data sets. In all data sets, however,  $k_{600}$  from anchored  
196 chambers ( $k_{600\_CO2\_a}$ ) differed significantly from that of drifting chambers (Fig. 1A). Except  
197 for data set A, both were weakly correlated to each other ( $r_S = 0.49$ ,  $p=0.01$  and  $r_S = 0.76$ ,  
198  $p<0.001$  for data set B and C, respectively) (Fig. 1B). With only a few exceptions, the gas

199 exchange velocities under anchored chambers were higher than those under drifting chambers,  
200 ~~with individual measurements,  $k_{600\_CO2\_a}$  being up to 20 times higher than  $k_{600\_CO2\_d}$ .~~ The  
201 average ratio of both velocities was 2.2, 6.2 and 4.0 for data set A, B and C, respectively  
202 (Table 2).

203 When both gases were measured, the gas exchange velocities estimated from  $\text{CO}_2$  fluxes were  
204 strongly correlated to those estimated from  $\text{CH}_4$  measurements for both deployment types.

205 Small but significant differences were observed between  $k_{600\_CO2\_d}$  and  $k_{600\_CH4\_d}$ , whereas the  
206  $\text{CO}_2$  based estimates were on average slightly higher in data set A and lower in data set B  
207 (Fig. 1A). In accordance with the  $\text{CO}_2$  based estimates,  $k_{600}$  estimated from  $\text{CH}_4$  was higher

208 under anchored than under drifting chambers (Table 2) and the ratio  $k_{600\_a} / k_{600\_d}$  did not  
209 differ significantly between both gases.

Gelöscht: measured

Feldfunktion geändert

Feldfunktion geändert

Feldfunktion geändert

Feldfunktion geändert

Gelöscht: .

Gelöscht: While

Gelöscht: in

Gelöscht: was

Gelöscht: .

Gelöscht: and t

Feldfunktion geändert

Feldfunktion geändert

Feldfunktion geändert

217 When combining all data sets, there was no correlation between gas exchange velocities and  
218 the measured current velocity for drifting chambers for either CO<sub>2</sub> or CH<sub>4</sub> (Fig. 2A).

Feldfunktion geändert

219 However, for anchored chamber deployments,  $k_{600_a}$  was positively correlated to current speed  
220 in data set A ( $r_S=0.54$ ,  $p=0.02$ ) and B ( $r_S=0.7$ ,  $p<0.001$ ). The ratio of the gas exchange  
221 velocities estimated from both deployment types was positively correlated to current speed  
222 when all three data sets were combined ( $r_S=0.66$ ,  $p<0.001$ ), but no significant correlations  
223 were observed within the individual data sets (Fig. 2B).

Feldfunktion geändert

224

### 225 3.2 Flow field and turbulence under chambers

226 The laboratory measurements revealed pronounced differences in the flow fields and  
227 turbulence under the anchored and drifting chambers. The mean longitudinal flow velocity  
228 was strongly reduced within the submerged part of the anchored chamber and increased  
229 below the submerged chamber edge. Recirculating eddies were formed under the leading  
230 (upstream) edge of the chamber (vector graphs of the mean velocity distributions are provided  
231 in Appendix B). These eddies detached and injected turbulence below the chamber (Fig. 3).

Feldfunktion geändert

Feldfunktion geändert

232 The turbulent kinetic energy which was produced by the submerged edge of the anchored  
233 chambers increased with increasing current speed (Appendix B). Under the drifting chambers,  
234 the flow velocities were slightly enhanced below the submerged chamber edge, but no  
235 recirculating eddies were formed.

Feldfunktion geändert

236 The penetration depth of the chamber edges varied with time as the chamber moved vertically  
237 on the rough water surface (see Appendix B for snapshots of instantaneous velocity  
238 distributions and chamber penetration). However, at the same flow velocity the average  
239 penetration depth of the anchored chamber was higher than that of the drifting chamber (Fig.  
240 3).

Feldfunktion geändert

Feldfunktion geändert

## 241 4 Discussion

### 242 4.1 Chamber bias in anchored deployments

243 Our field observations showed consistently higher gas exchange velocities and gas fluxes  
244 measured with anchored in comparison to freely drifting chambers in a variety of small  
245 streams with flow velocities between 0.08 and 0.8 m s<sup>-1</sup>. Detailed observations of the flow  
246 field and turbulence under both types of chambers in the laboratory revealed a reduction of  
247 mean flow velocity and the generation of chamber-induced turbulence due to the shedding of  
248 eddies at the upstream part of the submerged edge of the anchored chamber. Under identical  
249 hydraulic conditions, anchored chambers penetrated deeper into the water, which we attribute  
250 to a partial diversion of the strong horizontal drag force imposed by the flow into the vertical  
251 direction. In combination, horizontal current shear and deeper penetration caused an increase  
252 in magnitude of chamber-induced turbulence with increasing difference in velocity between  
253 the water flow and the chamber ([Fig. B1](#)). This mechanism has been suggested in previous  
254 studies of floating chamber performance in water bodies, although there are mixed results  
255 regarding its importance (Cole et al., 2010; Gålfalk et al., 2013; Vachon et al., 2010).  
256 The laboratory observation agrees with our field measurements, where the ratio of the fluxes  
257 measured with anchored and with drifting chambers was comparably small at flow velocities  
258 <0.2 m s<sup>-1</sup>. However, even at low flow velocities, the gas exchange velocity was enhanced by  
259 more than a factor of two in the anchored deployment. At higher flow velocities (> 0.2 m s<sup>-1</sup>)  
260 typical for rivers and streams, chamber-induced turbulence obviously dominated the gas flux  
261 into the anchored chambers.  
262 The large (several-fold) potential overestimation of fluxes measured with anchored chambers  
263 calls into question its suitability for application in running waters, particularly at high flow  
264 rates. This agrees with the observations of Teodoru et al. (2015) who reported a linear

Feldfunktion geändert

265 dependency of the gas exchange velocity under anchored chambers on the water velocity  
266 relative to the chamber in a large river.

#### 267 4.2 Correction methods and chamber optimization

268 The correlation of the anchored chamber gas exchange velocity with flow velocity observed  
269 in our study could provide a potential means for correcting the artificial chamber flux, if the  
270 corresponding drifting chamber gas exchange velocity was also a function of flow velocity.  
271 However, no such correlation was present in our field observations, indicating that near-  
272 surface flow velocity is a poor predictor for the gas exchange velocities in streams. Therefore,  
273 it can be expected that river depth and bed roughness affect the near-surface turbulence more  
274 than flow velocity (Moog and Jirka, 1999; Raymond et al., 2012).

275 As the correction of the effects of chamber-induced turbulence on measured fluxes seems  
276 unlikely, it would be more reasonable to optimize the chamber design to completely avoid or  
277 to at least reduce this effect. The rectangular chamber B produced the largest error, although it  
278 remained unclear from our measurements whether this was caused by the geometry of the  
279 chamber or by the high flow velocity in data set B. On this basis, we recommend the use of  
280 more streamlined circular chambers to minimize the error under drifting conditions. Crawford  
281 et al. (2013) and McMahon and Dennehy (1999) used streamlined (canoe-shaped) instead of  
282 cylindrical or rectangular chambers to minimize the generation of chamber-induced  
283 turbulence at the upstream chamber edge during anchored chamber deployments. However,  
284 they did not provide evidence that this goal was reached.

285 Another approach to minimize the bias of anchored chambers would be to design chambers  
286 without submerged rigid walls. Submergence of the chamber edges can be avoided  
287 completely by using a thin plastic foil which adheres to the water surface to seal the chamber  
288 headspace (Fig. 4A). Laboratory (PIV) measurements of the flow field were performed under  
289 a foil, mimicking a chamber deployed in anchored mode. The measurements revealed a strong

Feldfunktion geändert

290 reduction of flow disturbances and chamber-induced turbulence (Fig. 4) in comparison to  
291 both anchored and drifting chambers. Such “flying chambers” require a frame to keep the  
292 chamber above the water surface, which can be supported by floats at a larger lateral distance  
293 to the chamber or, in small streams, also by a fixation at the river bank.

294

#### 295 4.3 Implications for chamber-based flux measurements

296 Our study clearly shows that anchored chambers strongly overestimate the gas flux in running  
297 water and are not suited to quantify greenhouse gas fluxes in streams and rivers. One possible  
298 way forward to reduce this bias while still maintaining the practical advantages of the  
299 anchored chambers could be flying (anchored) chambers with flexible foil sealing at the water  
300 surface. Drifting chambers provide a practical and reliable solution, although they are not free  
301 of potential spatial bias. Because their measurement locations are difficult to control, their  
302 trajectories may not be representative for the areal mean flux from the study reach. Regions  
303 with locally enhanced turbulence, e.g., stream-reaches with large emerging roughness of the  
304 river bed, cannot be surveyed with drifting chambers, however the gas exchange velocity is  
305 highest at these sites (Moog and Jirka, 1999). Similarly, mean-flow trajectories may bypass  
306 backwaters and regions of reduced flow velocity along the stream banks. Observations in  
307 reservoirs and river impoundments revealed that the enhanced sedimentation of particulate  
308 organic matter can make these zones emission hot spots (Maeck et al., 2013; DelSontro et al.,  
309 2011). Anchored chamber deployments may provide a useful extension of drifting chamber  
310 measurements at such sites, if the flow velocity is sufficiently small. To truly validate a  
311 reliable chamber method for small streams, a multi-method comparison study, including  
312 tracer additions, should be performed.

313 This study shows that flux chamber approaches to measure GHG fluxes from running waters  
314 have a high potential, given sufficient knowledge about appropriate chamber design and

Feldfunktion geändert



315 deployment approaches. Thus, flux chambers are emerging as an important method to  
316 constrain greenhouse gas fluxes from stream networks.

317

## 318 Acknowledgments

319 Parts of this study were financially supported by the German Research Foundation (grant no.:  
320 LO 1150/9-1) and conducted within the *LandScales* project (*'Connecting processes and*  
321 *structures driving the landscape carbon dynamics over scales'*) financed by the the Leibniz  
322 Association within the Joint Initiative for Research and Innovation (BMBF) and (partially)  
323 carried out within the SMART Joint Doctorate (Science for the MAnagement of Rivers and  
324 their Tidal systems) funded with the support of the Erasmus Mundus program of the European  
325 Union and the Swiss National Science Foundation (Grant Nr. PA00P2\_142041). The  
326 development and production of the chambers with built in CO<sub>2</sub> loggers (data set C) was  
327 supported by the Swedish Research Council VR. Funding for an initial workshop was carried  
328 out by the IGB cross-cutting research domain 'Aquatic Boundaries and Linkages'. We  
329 gratefully acknowledge the financial support of German Academic Exchange Service  
330 (DAAD) (Sustainable water management Program (NAWAM), Grant number: A/12/91768).

331 We thank Simone Langhans for her fruitful input which shaped the core idea of the presented  
332 study. Finally, we thank the two anonymous reviewers for constructive inputs that improved  
333 the manuscript.

334

## 335 Appendices

### 336 Appendix A: Additional information on the field data sets

#### 337 A1: Data set A

338 Field measurements of five streams in North Central European Plains in Germany and Poland  
339 were conducted during October 2014. Gaseous CO<sub>2</sub> and CH<sub>4</sub> emissions were measured at the  
340 water-air interface with a drifting chamber attached to an Ultraportable Greenhouse Gas  
341 Analyzer (UGGA; Los Gatos Research, Inc., USA). The chamber was connected to the  
342 UGGA placed in a boat via two gas tight tubes (Tygon 2375), creating a circulation of air  
343 being sucked in and pumped out. For the anchored measurements, we tethered the chamber to  
344 a rack in the middle of the respective stream, in which we placed the sensors for continuously  
345 dissolved CO<sub>2</sub> and CH<sub>4</sub> measurements (HydroC™; CONTROS Systems & Solutions GmbH,  
346 Germany). Subsequently, we floated down a predefined stream section with the same  
347 chamber following freely the boat or vice versa at the speed of the current. During the  
348 chamber measurements, the UGGA continuously measured the gaseous CO<sub>2</sub> and CH<sub>4</sub>  
349 accumulation in the chamber (frequency 1 s). Flow velocity was measured with an Acoustic  
350 Digital Current Meter (OTT, Germany).

351

#### 352 A2: Data set B

353 Measurements were performed on the Bode River between EgelN-Nord and Staßfurt on 7  
354 April 2014 (summer base flow 7.7 m<sup>3</sup> s<sup>-1</sup>) and 12 March 2015 (winter high flow 12.8 m<sup>3</sup> s<sup>-1</sup>).  
355 The flux of CO<sub>2</sub> and CH<sub>4</sub> between water and atmosphere was measured by a rectangular  
356 floating chamber, which was connected to an FTIR analyzer (GASMET 4010, Finland).  
357 Measurements were performed from a boat while drifting down the river. For a single  
358 measurement, the chamber was placed at the water surface for up to five minutes and CO<sub>2</sub> and

359 CH<sub>4</sub> change inside the chamber was measured every 30 s. To compare drifting and fixed  
360 chamber measurements, the boat was then stopped by an anchor and measurements continued  
361 for another 3-5 min. During this stationary measurement, current velocity was measured with  
362 an electromagnetic current meter (MF-Pro, Ott, Germany) and water temperature were  
363 measured by hand held probes (ProfiLine Multi, WTW, Germany).  
364 The concentration of CO<sub>2</sub> in the water was continuously measured by a submersible probe  
365 (HydroC™; CONTROS Systems & Solutions GmbH, Germany). Additionally samples for  
366 CH<sub>4</sub> analysis were taken in plastic syringes and later analyzed by headspace GC.  
367 Water temperature was continuously measured by temperature loggers (Tidbit, Onset,  
368 U.S.A.). The barometric pressure was recorded by the FTIR analyzer.  
369 Under drifting conditions the CH<sub>4</sub> flux was often below the detection limit while there was  
370 always a positive CH<sub>4</sub> flux in anchored chamber deployments.

371

372 A3: Data set C

373 Chambers with a cross-sectional area of 0.066 m<sup>2</sup> and volume of 6.8 L were covered by  
374 aluminum foil to reduce the internal heating and equipped with a Styrofoam material to keep  
375 the chamber body floating on water surface. The chambers were equipped with an internal  
376 CO<sub>2</sub> logger system that is positioned inside the headspace of the chamber (Bastviken et al.,  
377 2015). The non-dispersive infrared (NDIR) CO<sub>2</sub> logger (ELG, SenseAir, Sweden,  
378 [www.senseair.se](http://www.senseair.se)) measures CO<sub>2</sub> in the range of 0-5000 ppm. The logger measures  
379 simultaneously CO<sub>2</sub>, temperature and relative humidity, and operates at temperature and  
380 humidity of 0-50 °C and 0-99% (non-condensing conditions) respectively. The loggers were  
381 calibrated by the manufacturer and operated with 9 VDC batteries. The measurement interval  
382 was adjusted to be 30 s, more information of technical specifications are provided elsewhere  
383 (Bastviken et al., 2015).

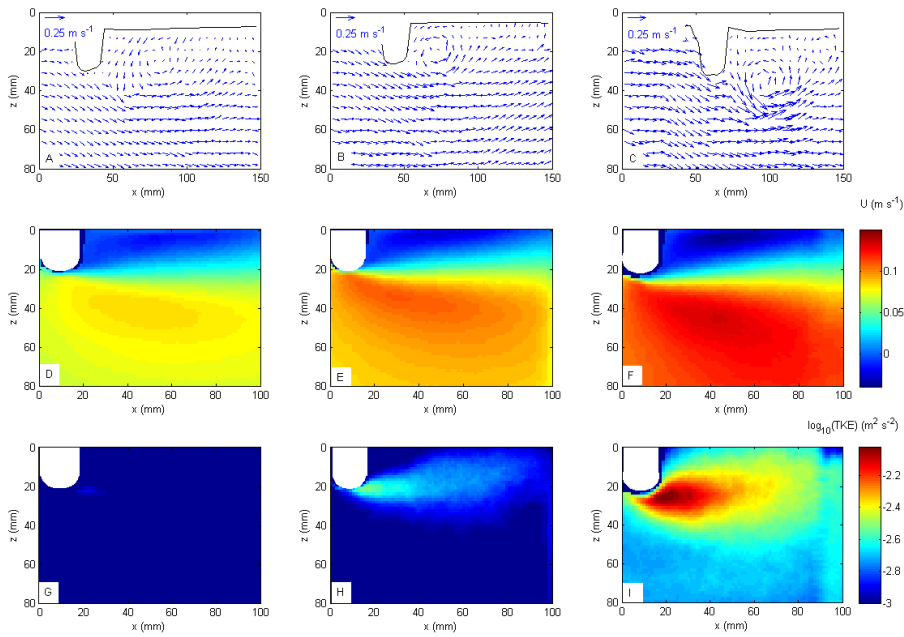
Gelöscht: for up to 5 minutes

Feldfunktion geändert

385 Chambers were deployed fixed at a certain position (anchored) and freely drifting. Triplicate  
386 measurements were conducted during each drifting run, and three runs were conducted at  
387 each site. The anchored chambers were then used for measuring the flux of CO<sub>2</sub> at different  
388 locations along the pathways of the drifting chambers. The chamber flux measurements were  
389 supplemented by measurements of dissolved gas CO<sub>2</sub> and CH<sub>4</sub> concentrations in the stream  
390 waters at each anchored stations for each run. Continuous measurements of CO<sub>2</sub> and methane  
391 in the middle of the stream were conducted using a membrane equilibrator (Liqui-Cel  
392 MiniModule, Membrana, USA) connected with an Ultraportable Greenhouse Gas Analyzer  
393 (UGGA; Los Gatos Research, Inc., USA). The water samples were pumped through the  
394 membrane contactor using a peristaltic pump at a constant flow rate.

395

396 Appendix B: Mean flow and turbulence under anchored chambers at different  
397 current speeds



398




399 **Fig. B1:** Laboratory measurements of flow velocity and turbulence under anchored chambers  
400 at different mean current speeds (left:  $0.06\text{ m s}^{-1}$ , middle:  $0.08\text{ m s}^{-1}$ , right:  $0.10\text{ m s}^{-1}$ . A-C)  
401 shows examples of instantaneous velocities around the leading edge of the chambers. The  
402 water surface and the leading chamber edge are marked by solid black lines. D-F) temporal  
403 mean longitudinal flow velocity ( $U$ ). G-I) mean turbulent kinetic energy (TKE). The chamber  
404 edges are masked out (white) and regions without sufficient observations ( $< 90\text{ s}$  for the  
405 anchored cases) are displayed in dark blue. The direction of flow was from left to right,  $x$  and  
406  $z$  refer to longitudinal distance and depth, respectively.

407 Tables

408 Table 1

409 **Table 1:** Summary of the three data sets obtained in field measurements. Pictures show the  
 410 three different chambers used for the anchored and drifting approach. Additional information  
 411 about the sampling procedures are provided in the [Supplementary Information](#).

Feldfunktion geändert

Data set	A	B	C
			
Site	5 different streams North-Central European Plains in Germany and Poland	Bode river, Harz mountains, Central Germany	3 different streams, Upper Rhine Valley, South-West Germany
Chamber volume (m <sup>3</sup> )	0.0168	0.0147	0.0068
Chamber area (m <sup>2</sup> ) (shape)	0.126 (circular)	0.098 (rectangular)	0.066 (circular)
Chamber height (m)	0.175	0.15	0.13
Penetration depth (m)	0.018	0.023	0.025
Chamber gas measurement	LosGatos, CO <sub>2</sub> , CH <sub>4</sub> on boat	FTIR analyzer (GASMET, Finland) on boat	Built-in low-cost CO <sub>2</sub> logger (ELG by SenseAir, Sweden)
Dissolved gas measurement	Contros CO <sub>2</sub> and CH <sub>4</sub>	Contros CO <sub>2</sub> , CH <sub>4</sub> with GC	UGGA with membrane contactor
Drifting measurements	following boat or vice versa	Freely drifting while followed with boat	Freely drifting
Anchored measurements	Tethered to a rack in the middle of the stream	Tethered to anchored boat	Tethered with rope from above
Number of measurements	At 5 sites: 2-5 pairs of anchored chamber measurements (upstream) and subsequent floating chamber runs	For two different discharge situations: 10-13 pairs of subsequent drifting and anchored chamber measurements down the river using a single chamber	At 3 sites: 2-3 subsequent floating chamber runs and 5 parallel anchored chambers distributed along the trajectory of the floating chamber

412 Table 2

413 **Table 2:** Discharge rate, flow velocities, gas fluxes ( $F_{\text{CO}_2}$ ,  $F_{\text{CH}_4}$ ), and gas exchange velocities  
414 ( $k_{600_{\text{CO}_2}}$ ,  $k_{600_{\text{CH}_4}}$ ) estimated from drifting (subscript d) and from anchored (subscript a)  
415 chambers during the three field campaigns (A-C, cf. [Table 1](#)). Except for discharge, all values  
416 are given as mean  $\pm$  standard deviation.

Data set	A	B	C
No. of samples $n$	$n_{\text{CO}_2}=18$ $n_{\text{CH}_4}=18$	$n_{\text{CO}_2}=27$ $n_{\text{CH}_4}=9$	$n_{\text{CO}_2}=24$ $n_{\text{CH}_4}=0$
<u>Discharge (<math>\text{m}^3 \text{s}^{-1}</math>)</u>	<u>0.6 – 1.4</u>	<u>7.7 – 12.8</u>	<u>0.1 – 7.6</u>
Flow velocity ( $\text{m s}^{-1}$ )	$0.21 \pm 0.07$	$0.60 \pm 0.12$	$0.30 \pm 0.07$
$F_{\text{CO}_2_{\text{a}}}$ ( $\text{mmol m}^{-2} \text{day}^{-1}$ )	$742 \pm 282$	$302 \pm 148$	$103 \pm 47$
$F_{\text{CO}_2_{\text{d}}}$ ( $\text{mmol m}^{-2} \text{day}^{-1}$ )	$363 \pm 139$	$55 \pm 30$	$49 \pm 36$
$k_{600_{\text{CO}_2_{\text{a}}}}$ ( $\text{m day}^{-1}$ )	$6.5 \pm 1.4$	$17 \pm 6.4$	$4.1 \pm 2.8$
$k_{600_{\text{CO}_2_{\text{d}}}}$ ( $\text{m day}^{-1}$ )	$3.3 \pm 1.1$	$3.2 \pm 1.5$	$2.1 \pm 2.5$
$k_{600_{\text{CO}_2_{\text{a}}}} / k_{600_{\text{CO}_2_{\text{d}}}}$	$2.2 \pm 0.9$	$6.2 \pm 3.2$	$4.0 \pm 5.0$
$F_{\text{CH}_4_{\text{a}}}$ ( $\text{mmol m}^{-2} \text{day}^{-1}$ )	$4.31 \pm 1.35$	$1.55 \pm 0.71$	-
$F_{\text{CH}_4_{\text{d}}}$ ( $\text{mmol m}^{-2} \text{day}^{-1}$ )	$2.12 \pm 0.86$	$0.37 \pm 0.16$	-
$k_{600_{\text{CH}_4_{\text{a}}}}$ ( $\text{m day}^{-1}$ )	$6.0 \pm 1.4$	$23.0 \pm 10.8$	-
$k_{600_{\text{CH}_4_{\text{d}}}}$ ( $\text{m day}^{-1}$ )	$2.9 \pm 0.9$	$5.5 \pm 2.4$	-
$k_{600_{\text{CH}_4_{\text{a}}}} / k_{600_{\text{CH}_4_{\text{d}}}}$	$2.3 \pm 1.0$	$4.8 \pm 2.1$	-

417

Gelöscht: F

Gelöscht: A

Feldfunktion geändert

Gelöscht: .

Formatiert: Schriftart: Nicht Fett

Formatiert: Links

Formatiert: Hochgestellt

Formatiert: Schriftart: Nicht Fett

421 Figures

422 Figure 1

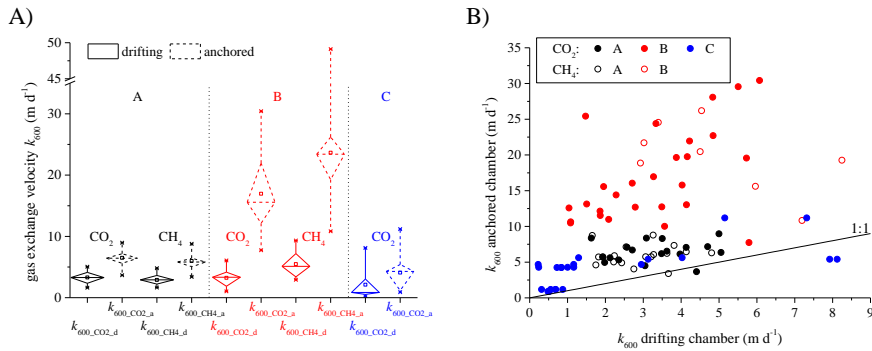
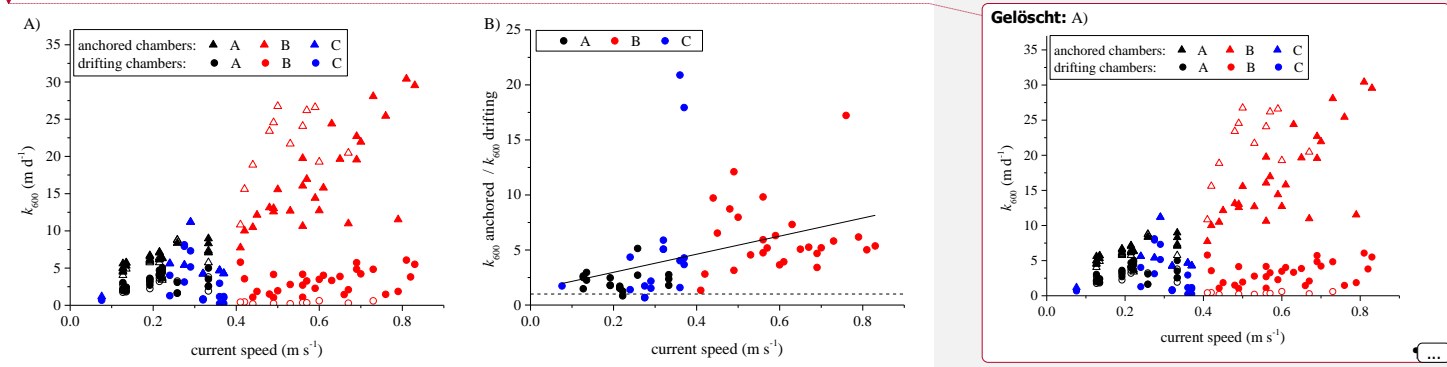


**Fig. 1:** A) Box plots of the standardized gas exchange ( $k_{600}$ ) velocity measured using drifting (solid lines) and anchored (dashed lines) flux chambers in data set A (black), B (red) and C (blue). The diamond-shaped boxes encompass the 25-75 percentile range, whiskers show minimum and maximum, open squares and horizontal lines mark mean and median values, respectively. B)  $k_{600}$  estimated from anchored chamber deployments versus that from drifting chambers for the data sets A-C (color). Filled symbols show  $k_{600}$  estimated from CO<sub>2</sub> fluxes, open symbols are based on CH<sub>4</sub> fluxes. The solid line shows a 1:1 relationship.

423

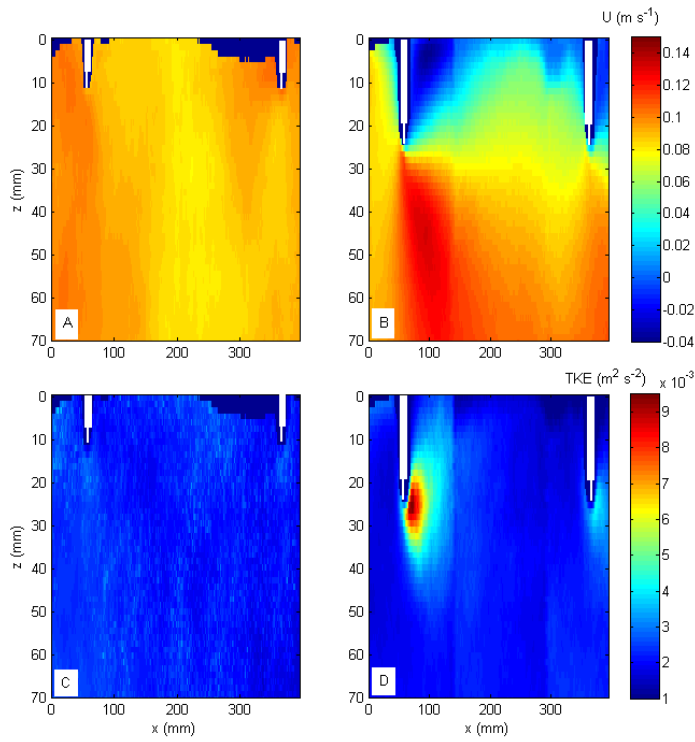


424 Figure 2



425  
426 **Fig. 2:** A) Gas exchange velocity  $k_{600}$  from anchored (triangles) and drifting  
427 chambers versus current velocity for the three field data sets (A-C, colors). Filled symbols  
428 show data obtained from CO<sub>2</sub>, open symbols are based on CH<sub>4</sub> fluxes. B) Ratio of the gas  
429 exchange velocities from anchored and drifting chambers versus current speed (filled  
430 symbols: CO<sub>2</sub>, open symbols: CH<sub>4</sub>, symbol color indicates data set). The dashed line indicates  
431 a constant ratio of one and the solid line shows a linear regression of the combined data sets  
432 ( $r_s=0.66, p<0.001$ ).

435 Figure 3



436

437 **Fig. 3:** Laboratory measurements of the mean longitudinal flow velocities ( $U$ ) A) below a  
438 drifting and B) below an anchored chamber. Mean turbulent kinetic energy (TKE) of the flow  
439 fields below C) the drifting chamber and D) the anchored chamber.  $z$  and  $x$  refer to depth and  
440 longitudinal distance respectively. Chamber edges are masked out (white) and regions without  
441 sufficient observations for temporal averaging are marked by dark blue color. The flow  
442 direction is from left to right and the mean flow velocity was 0.1 m s<sup>-1</sup>.

443

444 Figure 4

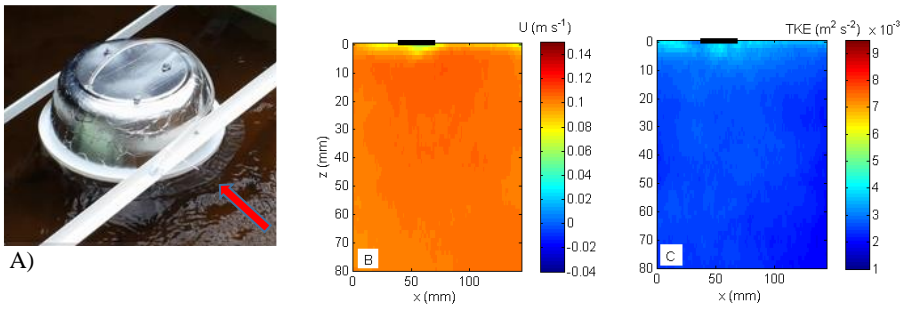


**Fig. 4:** A) Flying chamber design without penetration of the water surface by the chamber edges but using a plastic foil collar (marked by the red arrow) for sealing. The chamber is fixed above the water surface by a supporting frame. B) Distribution of mean longitudinal flow velocities ( $U$ ) and C) turbulent kinetic energy ( $TKE$ ) of the flow field below the front edge of a static foil (marked by black bar) at the water surface. The direction of flow was from left to right,  $x$  and  $y$  refer to longitudinal distance and depth, respectively. The mean flow velocity was  $0.10 \text{ m s}^{-1}$ . Color scales are identical to that of Fig. 3.

445

## 446 References

- 447 Alin, S. R., Rasera, M., Salimon, C. I., Richey, J. E., Holtgrieve, G. W., Krusche, A. V., and  
448 Snidvongs, A.: Physical controls on carbon dioxide transfer velocity and flux in low-  
449 gradient river systems and implications for regional carbon budgets, *J. Geophys. Res.-*  
450 *Biogeo.*, 116, G01009, 10.1029/2010jg001398, 2011.
- 451 Aufdenkampe, A. K., Mayorga, E., Raymond, P. A., Melack, J. M., Doney, S. C., Alin, S. R.,  
452 Aalto, R. E., and Yoo, K.: Riverine coupling of biogeochemical cycles between land,  
453 oceans, and atmosphere, *Front. Ecol. Environ.*, 9, 53-60, 10.1890/100014, 2011.
- 454 Baldocchi, D.: Measuring fluxes of trace gases and energy between ecosystems and the  
455 atmosphere – the state and future of the eddy covariance method, *Global Change Biol.*,  
456 20, 3600-3609, 10.1111/gcb.12649, 2014.
- 457 Bastviken, D., Tranvik, L. J., Downing, J. A., Crill, P. M., and Enrich-Prast, A.: Freshwater  
458 Methane Emissions Offset the Continental Carbon Sink, *Science*, 331, 50-50,  
459 10.1126/science.1196808, 2011.
- 460 Bastviken, D., Sundgren, I., Natchimuthu, S., Reyier, H., and Gålfalk, M.: Technical Note:  
461 Cost-efficient approaches to measure carbon dioxide (CO<sub>2</sub>) fluxes and concentrations in  
462 terrestrial and aquatic environments using mini loggers, *Biogeosciences*, 12, 3849-3859,  
463 10.5194/bg-12-3849-2015, 2015.
- 464 Battin, T. J., Kaplan, L. A., Findlay, S., Hopkinson, C. S., Marti, E., Packman, A. I.,  
465 Newbold, J. D., and Sabater, F.: Biophysical controls on organic carbon fluxes in fluvial  
466 networks, *Nature Geosci.*, 1, 95-100, 10.1038/ngeo101, 2008.
- 467 Beaulieu, J. J., Shuster, W. D., and Rebolz, J. A.: Controls on gas transfer velocities in a  
468 large river, *J. Geophys. Res.-Biogeo.*, 117, G02007, 10.1029/2011jg001794, 2012.
- 469 Beaulieu, J. J., Smolenski, R. L., Nietch, C. T., Townsend-Small, A., and Elovitz, M. S.: High  
470 Methane Emissions from a Midlatitude Reservoir Draining an Agricultural Watershed,  
471 *Environ. Sci. Technol.*, 48, 11100-11108, 10.1021/es501871g, 2014.
- 472 Butman, D., and Raymond, P. A.: Significant efflux of carbon dioxide from streams and  
473 rivers in the United States, *Nature Geosci.*, 4, 839-842, 2011.
- 474 Campeau, A., and Del Giorgio, P. A.: Patterns in CH<sub>4</sub> and CO<sub>2</sub> concentrations across boreal  
475 rivers: Major drivers and implications for fluvial greenhouse emissions under climate  
476 change scenarios, *Glob Chang Biol*, 20, 1075-1088, 2014.
- 477 Cole, J. J., Prairie, Y. T., Caraco, N. F., McDowell, W. H., Tranvik, L. J., Striegl, R. G.,  
478 Duarte, C. M., Kortelainen, P., Downing, J. A., Middelburg, J. J., and Melack, J.:  
479 Plumbing the global carbon cycle: Integrating inland waters into the terrestrial carbon  
480 budget, *Ecosystems*, 10, 171-184, 10.1007/s10021-006-9013-8, 2007.
- 481 Cole, J. J., Bade, D. L., Bastviken, D., Pace, M. L., and Van de Bogert, M.: Multiple  
482 approaches to estimating air-water gas exchange in small lakes, *Limnol. Oceanogr.*  
483 *Meth.*, 8, 285-293, 10.4319/lom.2010.8.285, 2010.
- 484 Crawford, J. T., Striegl, R. G., Wickland, K. P., Dornblaser, M. M., and Stanley, E. H.:  
485 Emissions of carbon dioxide and methane from a headwater stream network of interior  
486 Alaska, *J. Geophys. Res.-Biogeo.*, 118, 482-494, 10.1002/jgrg.20034, 2013.
- 487 DelSontro, T., Kunz, M. J., Kempter, T., Wüest, A., Wehrli, B., and Senn, D. B.: Spatial  
488 Heterogeneity of Methane Ebullition in a Large Tropical Reservoir, *Environ. Sci.*  
489 *Technol.*, 45, 9866-9873, 10.1021/es2005545, 2011.
- 490 Eugster, W., DelSontro, T., and Sobek, S.: Eddy covariance flux measurements confirm  
491 extreme CH<sub>4</sub> emissions from a Swiss hydropower reservoir and resolve their short-term  
492 variability, *Biogeosciences*, 8, 2815-2831, 10.5194/bg-8-2815-2011, 2011.

Formatiert: Englisch (USA)

493 Gålfalk, M., Bastviken, D., Fredriksson, S., and Arneborg, L.: Determination of the piston  
494 velocity for water-air interfaces using flux chambers, acoustic Doppler velocimetry, and  
495 IR imaging of the water surface, *J. Geophys. Res.-Biogeo.*, 118, 770-782,  
496 10.1002/jgrg.20064, 2013.

497 Goldenfum, J. A.: GHG Measurement Guidelines for Freshwater Reservoirs, UNESCO/IHA,  
498 London, 139 pp., 2011.

499 Halbedel, S., and Koschorreck, M.: Regulation of CO<sub>2</sub> emissions from temperate streams and  
500 reservoirs, *Biogeosciences*, 10, 7539-7551, 10.5194/bg-10-7539-2013, 2013.

501 Hotchkiss, E. R., Hall Jr, R. O., Sponseller, R. A., Butman, D., Klaminder, J., Laudon, H.,  
502 Rosvall, M., and Karlsson, J.: Sources of and processes controlling CO<sub>2</sub> emissions  
503 change with the size of streams and rivers, *Nature Geosci.*, 8, 696-699,  
504 10.1038/ngeo2507, 2015.

505 Jähne, B., and Haußecker, H.: Air-water gas exchange, *Ann. Rev. Fluid Mech.*, 30, 443-468,  
506 1998.

507 Koprivnjak, J. F., Dillon, P. J., and Molot, L. A.: Importance of CO<sub>2</sub> evasion from small  
508 boreal streams, *Global Biogeochem. Cycles*, 24, Gb4003, 10.1029/2009gb003723, 2010.

509 Kremer, J. N., Nixon, S. W., Buckley, B., and Roques, P.: Technical Note: Conditions for  
510 Using the Floating Chamber Method to Estimate Air-Water Gas Exchange, *Estuaries*, 26,  
511 985-990, 10.1007/BF02803357, 2003.

512 Le Quéré, C., Peters, G. P., Andres, R. J., Andrew, R. M., Boden, T. A., Ciais, P.,  
513 Friedlingstein, P., Houghton, R. A., Marland, G., Moriarty, R., Sitch, S., Tans, P., Arneeth,  
514 A., Arvanitis, A., Bakker, D. C. E., Bopp, L., Canadell, J. G., Chini, L. P., Doney, S. C.,  
515 Harper, A., Harris, I., House, J. I., Jain, A. K., Jones, S. D., Kato, E., Keeling, R. F.,  
516 Klein Goldewijk, K., Körtzinger, A., Koven, C., Lefèvre, N., Maignan, F., Omar, A.,  
517 Ono, T., Park, G. H., Pfeil, B., Poulter, B., Raupach, M. R., Regnier, P., Rödenbeck, C.,  
518 Saito, S., Schwinger, J., Segschneider, J., Stocker, B. D., Takahashi, T., Tilbrook, B., van  
519 Heuven, S., Viovy, N., Wanninkhof, R., Wiltshire, A., and Zaehle, S.: Global carbon  
520 budget 2013, *Earth Syst. Sci. Data*, 6, 235-263, 10.5194/essd-6-235-2014, 2014.

521 Maeck, A., DelSontro, T., McGinnis, D. F., Fischer, H., Flury, S., Schmidt, M., Fietzek, P.,  
522 and Lorke, A.: Sediment trapping by dams creates methane emission hotspots, *Environ.*  
523 *Sci. Technol.*, 47, 8130-8137, 2013.

524 Marion, A., Nikora, V., Puijalón, S., Bouma, T., Koll, K., Ballio, F., Tait, S., Zaramella, M.,  
525 Sukhodolov, A., O'Hare, M., Wharton, G., Aberle, J., Tregnaghi, M., Davies, P., Nepf,  
526 H., Parker, G., and Statzner, B.: Aquatic interfaces: a hydrodynamic and ecological  
527 perspective, *J. Hydraul. Res.*, 1-15, 10.1080/00221686.2014.968887, 2014.

528 McMahon, P. B., and Dennehy, K. F.: N<sub>2</sub>O emissions from a nitrogen-enriched river,  
529 *Environ. Sci. Technol.*, 33, 21-25, 10.1021/es980645n, 1999.

530 Moog, D., and Jirka, G.: Stream Reaeration in Nonuniform Flow: Macroroughness  
531 Enhancement, *J. Hydraul. Eng.*, 125, 11-16, doi:10.1061/(ASCE)0733-  
532 9429(1999)125:1(11), 1999.

533 Raymond, P. A., and Cole, J. J.: Gas exchange in rivers and estuaries: Choosing a gas transfer  
534 velocity, *Estuaries*, 24, 312-317, 10.2307/1352954, 2001.

535 Raymond, P. A., Zappa, C. J., Butman, D., Bott, T. L., Potter, J., Mulholland, P., Laursen, A.  
536 E., McDowell, W. H., and Newbold, D.: Scaling the gas transfer velocity and hydraulic  
537 geometry in streams and small rivers, *Limnology & Oceanography: Fluids &*  
538 *Environments*, 2, 41-53, 10.1215/21573689-1597669, 2012.

539 Raymond, P. A., Hartmann, J., Lauerwald, R., Sobek, S., McDonald, C., Hoover, M.,  
540 Butman, D., Striegl, R., Mayorga, E., Humborg, C., Kortelainen, P., Durr, H., Meybeck,  
541 M., Ciais, P., and Guth, P.: Global carbon dioxide emissions from inland waters, *Nature*,  
542 503, 355-359, 10.1038/nature12760, 2013.

543 Sand-Jensen, K., and Staehr, P.: CO<sub>2</sub> dynamics along Danish lowland streams: water–air  
544 gradients, piston velocities and evasion rates, *Biogeochemistry*, 111, 615–628,  
545 10.1007/s10533-011-9696-6, 2012.

546 Teodoru, C. R., Nyoni, F. C., Borges, A. V., Darchambeau, F., Nyambe, I., and Bouillon, S.:  
547 Dynamics of greenhouse gases (CO<sub>2</sub>, CH<sub>4</sub>, N<sub>2</sub>O) along the Zambezi River and major  
548 tributaries, and their importance in the riverine carbon budget, *Biogeosciences*, 12, 2431–  
549 2453, 10.5194/bg-12-2431-2015, 2015.

550 Tranvik, L. J., Downing, J. A., Cotner, J. B., Loiselle, S. A., Striegl, R. G., Ballatore, T. J.,  
551 Dillon, P., Finlay, K., Fortino, K., Knoll, L. B., Kortelainen, P. L., Kutser, T., Larsen, S.,  
552 Laurion, I., Leech, D. M., McCallister, S. L., McKnight, D. M., Melack, J. M., Overholt,  
553 E., Porter, J. A., Prairie, Y., Renwick, W. H., Roland, F., Sherman, B. S., Schindler, D.  
554 W., Sobek, S., Tremblay, A., Vanni, M. J., Verschoor, A. M., von Wachenfeldt, E., and  
555 Weyhenmeyer, G. A.: Lakes and reservoirs as regulators of carbon cycling and climate,  
556 *Limnol. Oceanogr.*, 54, 2298–2314, 10.4319/lo.2009.54.6\_part\_2.2298, 2009.

557 Vachon, D., Prairie, Y. T., and Cole, J. J.: The relationship between near-surface turbulence  
558 and gas transfer velocity in freshwater systems and its implications for floating chamber  
559 measurements of gas exchange, *Limnol. Oceanogr.*, 55, 1723–1732,  
560 10.4319/lo.2010.55.4.1723, 2010.

561 Wallin, M. B., Oquist, M. G., Buffam, I., Billett, M. F., Nisell, J., and Bishop, K. H.:  
562 Spatiotemporal variability of the gas transfer coefficient ( $K(\text{CO}_2)$ ) in boreal streams:  
563 Implications for large scale estimates of CO<sub>2</sub> evasion, *Global Biogeochem. Cycles*, 25,  
564 Gb3025, 10.1029/2010gb003975, 2011.

565